

# Unsteady Couette Flow in a Composite Channel Partially Filled with Porous Material: A Semi-analytical Approach

Basant K. Jha · J. O. Odengle

Received: 4 June 2014 / Accepted: 1 December 2014 / Published online: 6 December 2014  
© Springer Science+Business Media Dordrecht 2014

**Abstract** This study is devoted to investigate the unsteady fully developed time-dependent Couette flow in a composite channel partially filled with porous material. The Brinkman-extended Darcy model is used to simulate momentum transfer in the porous medium. The fluid and porous regions are interlinked by equating the velocity and by considering shear stress jump conditions in the interface. The solutions of the governing equations are obtained using a Laplace transform technique. However, the Riemann-sum approximation method is used to invert from Laplace domain to time domain. The solution obtained is validated by presenting comparisons with closed form solution obtained for steady flow which has been derived separately and also by implicit finite difference method. During the course of numerical comparison, an excellent agreement was found between steady-state solution obtained exactly and unsteady solution obtained by implicit finite difference method or Riemann-sum approximation method at large values of time. The effect of various flow parameters entering into the problem is discussed with the aid of line graphs. The results obtained here may be further used to verify the validity of obtained numerical solutions for more complicated time-dependent Couette flow in composite channel.

**Keywords** Unsteady Couette flow · Riemann-sum approximation · Composite channel

## List of Symbols

- $d'$  Dimensional thickness of clear fluid region
- $d$  Dimensionless thickness of clear fluid
- $y'$  Coordinate normal to the plates
- $y$  Dimensionless coordinate normal to the plates

---

B. K. Jha  
Department of Mathematics, Ahmadu Bello University, Zaria, Nigeria

J. O. Odengle (✉)  
Iya Abubakar Computer Centre, Ahmadu Bello University, Zaria, Nigeria  
e-mail: odengle\_jo@yahoo.com

|        |   |
|--------|---|
| $H$    | Distance between the two infinite parallel plates |
| $Da$   | Darcy number                                      |
| $u'$   | Fluid velocity in dimensional form                |
| $u$    | Fluid velocity in dimensionless form              |
| $U'_i$ | Interfacial velocity in dimensional form          |
| $U_i$  | Interfacial velocity in dimensionless form        |
| $t'$   | Time in dimensional form                          |
| $t$    | Time in dimensionless form                        |
| $k$    | Permeability of the porous medium                 |

## Greek Symbols

|                    |   |
|--------------------|---|
| $\nu_{\text{eff}}$ | Effective kinematic viscosity of the porous medium  |
| $\nu$              | Kinematics viscosity of the fluid                   |
| $\beta$            | Adjustable coefficient in the stress jump condition |
| $\gamma$           | Ratio of viscosities                                |

## Subscripts

|   |  |
|---|--|
| f | Fluid region                                     |
| p | Porous region                                    |
| i | Interface between clear fluid and porous regions |

## 1 Introduction

Fluid flow in composite channel has continued to attract interest because of its practical applications in geophysical environments and industries. These include engineering applications such as thermal-energy storage system, crude oil extraction, and cores of nuclear reactors.

[Beavers and Joseph \(1967\)](#) first studied the flow mechanism at porous/fluid interface utilizing the Darcy law to model flow in porous region. [Neale and Nader \(1974\)](#) showed that for the flow in a channel having fluid and porous region, the Darcy model with the Beavers-Joseph condition gives the same result as that obtained by using the Brinkman model when continuity of the velocity and shear stress at the interface is considered. [Vafai and Kim \(1990\)](#) revisited the work of [Beavers and Joseph \(1967\)](#) and obtained an exact solution describing the interfacial mechanics. [Kuznetsov \(1996\)](#) also carried out investigation of steady fluid flow in the interface region between a porous medium and clear fluid in channels partially filled with a porous medium by considering three different channels. Latter, [Kuznetsov \(1997\)](#) worked on the influence of the stress jump condition at the porous medium/clear fluid interface in a composite channel in steady-state operating condition.

[Paul and Singh \(1998\)](#) studied steady fully developed natural convection between coaxial vertical cylinders partially filled with a porous material. [Paul et al. \(1999\)](#) then worked on transient natural convection in a vertical channel partially filled with a porous medium using numerical method. [Al-Nimr and Alkam \(1998\)](#) used Green's function method to obtain analytical solutions for problems of transient fluid flow in parallel-plate channels partially filled with porous material. The work of [Hajipour and Dehkordi \(2012\)](#) focused on the effect of inertial term and viscous dissipation on transient fluid flow and heat transfer in vertical channel partially filled with porous medium using numerical method. In another paper, [Hajipour](#)

and Dehkordi (2011) considered mixed convective heat transfer of nanofluids in a parallel-plate channel partially filled with a porous material analytically and numerically for constant temperature boundary condition. The transient and non-Darcian effects on natural convection fluid flow in a vertical channel partially filled with porous medium are studied by Singh (2011). Singh and Gorla (2008) in their work on heat transfer between two vertical parallel walls partially filled with porous material, observed that for large values of Darcy number, the effect of Brinkman term is on the entire porous domain, while for small values of Darcy number, its effect is confined in the vicinity of the interface only. Jaballah et al. (2008) treated the numerical simulation of the heat transfer and the mixed convection of an incompressible fluid filling a horizontal channel, where some porous blocks were intermittently inserted transverse to the channel axis. Singh (2011) considered transient and non-Darcian effects on natural convection flow in a vertical channel partially filled with porous medium using the Forchheimer-Brinkman-extended Darcy model.

According to Muzychka and Youanovich (2006), Couette flow can be used as a fundamental method for the measurement of viscosity and as a means of estimating the drag force in many wall-driven applications. The case of heat transfer in Couette flow through a porous medium using a Brinkman-Darcy porous medium is investigated by Bhargava and Sacheti (1989). In a similar work, Daskalakis (1990) considered heat transfer in Couette flow through a porous medium of high Prandtl number fluid with temperature-dependent viscosity. Ochoa-Tapia and Whitaker (1995a, b) studied momentum transfer at the boundary between a porous medium and a homogeneous fluid. Kuznetsov (1998) utilized the boundary conditions at the interface suggested in Ochoa-Tapia and Whitaker to investigate Couette flow in a composite channel partially filled with a porous medium and partially with a clear fluid. Jain et al. (2006) studied Couette flow through a highly porous medium between two horizontal parallel porous flat plates with transverse sinusoidal injection of the fluid at the stationary plate and its corresponding removal by constant suction through the moving plate in a uniform motion. The effect of transpiration on free convective Couette flow in a composite channel was investigated by Jha et al. (2011). The paper concentrated on the analytical investigation of steady-state convective Couette flow of fluid between two vertical parallel plates partially filled with porous medium and partially with clear fluid in the presence of suction / injection.

The objective of this work is to analyze unsteady Couette flow in a composite channel partially filled with porous material using a semi-analytical approach which to the best knowledge of the authors has not been done yet. This study is limited to the fluid-flow analysis only. In it, the solutions of the governing equations are obtained by using a Laplace transform technique, while the Riemann-sum approximation method is used to invert the Laplace domain to the time domain.

## 2 Mathematical Analysis

We considered unsteady Couette flow in a composite channel bounded by two infinite horizontal parallel plates as shown in Fig. 1

The gap between the plates is  $H$ . The lower part of the channel is occupied by clear fluid ( $0 \leq y' \leq d'$ ), while the upper part ( $d' \leq y' \leq H$ ) is occupied by a fully saturated porous medium with uniform permeability.

The direction of the flow is taken along the horizontal  $x'$ -axis, while the  $y'$ -axis is taken perpendicular to it. At time  $t' \leq 0$ , the fluid and the plate are assumed to be at rest. At time  $t' > 0$ , the lower plate begins to move in its own plane with a constant velocity  $U_0$ . The governing equations in dimensional form are given as

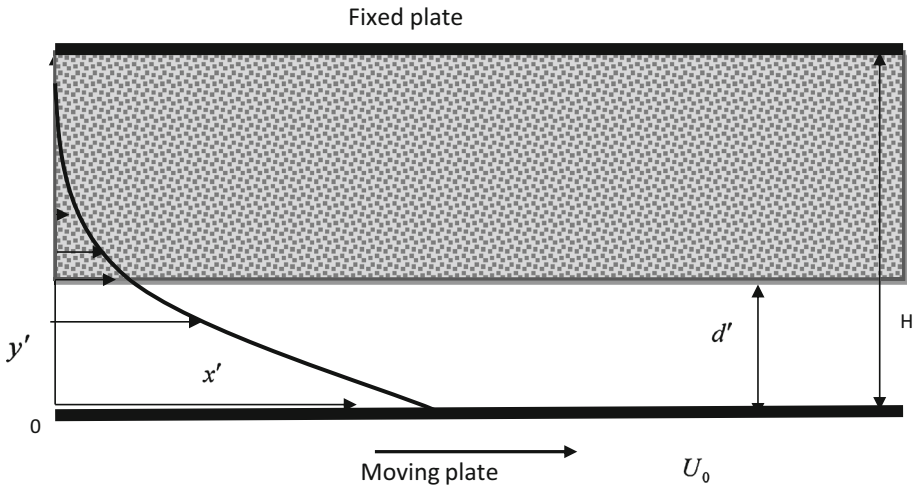


**Fig. 1** Geometrical illustration of the problem

$$\frac{\partial u'}{\partial t'} = \nu \frac{\partial^2 u'_f}{\partial y'^2} \tag{1}$$

$$\frac{\partial u'_p}{\partial t'} = \nu_{\text{eff}} \frac{\partial^2 u'_p}{\partial y'^2} - \nu \frac{u'_p}{k} \tag{2}$$

The initial and boundary conditions in dimensional form are

$$\begin{aligned} t' \leq 0 : u'_f = u'_p = 0 \quad \text{for } 0 \leq y' \leq H \\ t' > 0 : \left[ \begin{array}{l} u'_f = U_0, \quad \text{at } y' = 0; \\ u'_p = 0, \quad \text{at } y' = H. \end{array} \right] \\ t' > 0 : y' = d' \left[ \begin{array}{l} u'_f = u'_p = U'_i; \\ \nu_{\text{eff}} \frac{\partial u'_p}{\partial y'} - \nu \frac{\partial u'_f}{\partial y'} = \frac{\beta \nu u'_p}{\sqrt{k}}. \end{array} \right] \end{aligned} \tag{3}$$

Introducing the following dimensionless quantities in Eq. (1)–(3),

$$\begin{aligned} y = \frac{y'}{H}; \quad \gamma = \frac{\nu_{\text{eff}}}{\nu}; \quad d = \frac{d'}{H}; \quad Da = \frac{k}{H^2}; \quad u_p = \frac{u'_p}{U_0}; \\ u_f = \frac{u'_f}{U_0}; \quad U_i = \frac{U'_i}{U_0}; \quad t = \frac{t' \nu}{H^2} \end{aligned}$$

Equations (1) and (2) can then be written in dimensionless form as

$$\frac{\partial u_f}{\partial t} = \frac{\partial^2 u_f}{\partial y^2} \tag{4}$$

$$\frac{\partial u_p}{\partial t} = \gamma \frac{\partial^2 u_p}{\partial y^2} - \frac{u_p}{Da} \tag{5}$$

subject to the following dimensionless initial and boundary conditions:

$$\begin{aligned}
 t' \leq 0 : u_f = u_p = 0, \quad \text{for } 0 \leq y \leq 1 \\
 t > 0 : \begin{cases} u_f = 1, & \text{at } y = 0 \\ u_p = 0, & \text{at } y = 1 \end{cases} \\
 t > 0 : y = d : \left[ u_f = u_p = U_i \right. \\
 \left. \gamma \frac{du_p}{dy} - \frac{du_f}{dy} = \frac{\beta}{\sqrt{Da}} u_p \right]
 \end{aligned} \tag{6}$$

The solutions of Eqs. (4) and (5) can be obtained using the Laplace transforms technique. Define the following transform variables:

$$\bar{u}(y, s) = \int_0^\infty u(y, t)e^{-st} dt,$$

where  $s$  is the Laplace parameter and  $s > 0$ . Taking the Laplace transform of Eq. (4) and (5),

$$\frac{d^2 \bar{u}_f}{dy^2} - s \bar{u}_f = 0 \tag{7}$$

$$\frac{d^2 \bar{u}_p}{dy^2} - \left( \frac{s + \frac{1}{Da}}{\gamma} \right) \bar{u}_p = 0 \tag{8}$$

The solutions of Eqs. (7) and (8) are, respectively,

$$\bar{u}_f(y, s) = \frac{1}{s} \frac{\sinh((d-y)\sqrt{s})}{\sinh(d\sqrt{s})} + \frac{U_i \sinh(y\sqrt{s})}{s \sinh(d\sqrt{s})} \tag{9}$$

$$\bar{u}_p(y, s) = \frac{U_i \sinh(F(y-1))}{s \sinh(F(d-1))}, \tag{10}$$

where

$$F = \sqrt{\frac{s + \frac{1}{Da}}{\gamma}}; \quad U_i = \frac{\frac{1}{\sqrt{s}} \sinh(d\sqrt{s}) - x_5 \sqrt{s} \cosh(d\sqrt{s})}{x_2 x_3 - x_1 x_4 - \sqrt{s} \cosh(d\sqrt{s}) x_6};$$

$$x_1 = \gamma F \sinh(dF) - \frac{\beta}{\sqrt{Da}} \cosh(dF); \quad x_2 = \gamma F \cosh(dF) - \frac{\beta}{\sqrt{Da}} \sinh(dF);$$

$$x_3 = \frac{\cosh(F)}{\sinh(F(d-1))}; \quad x_4 = \frac{\sinh(F)}{\sinh(F(d-1))}; \quad x_5 = \frac{1 \cosh(d\sqrt{s})}{s \sinh(d\sqrt{s})};$$

$$x_6 = \frac{1}{\sinh(d\sqrt{s})}.$$

Equations (9) and (10) are then inverted in order to determine the velocities in the time domain. The numerical procedure used in Jha et al. (2011) and Khadrawi and Al-Nimr (2007) which is based on the Riemann-sum approximation is applied to find the inverse of Eqs. (9) and (10). In this method, functions in the Laplace domain can be transformed to the time domain as follows:

$$u(y, t) = \frac{e^{\epsilon t}}{t} \left[ \frac{1}{2} \bar{u}(y, \epsilon) + Re \sum_{k=1}^N \bar{u} \left( y, \epsilon + \frac{ik\pi}{t} \right) (-1)^k \right] \tag{11}$$

where  $Re$  is ‘‘real part of,’’  $i = \sqrt{-1}$ , the imaginary number,  $N$  is the number of terms used in the Riemann-sum approximation, and is the real part of the Bromwich contour that is used

in inverting Laplace transforms. The Riemann-sum approximation for the Laplace inversion involves a single summation for the numerical process. Its accuracy depends on the value of  $\epsilon$  and the truncation error dictated by  $N$ . In the work of Tzou (1997) the value of  $\epsilon t$  that best satisfied the result is 4.7.

### 2.1 Skin Friction and Volumetric Flow Rate

The skin friction at  $y = 0$ ,  $\tau_0(y, s)$ , and  $y = 1$ ,  $\tau_1(y, s)$  in terms of the Laplace parameter  $s$  is computed by differentiating Eq. (9) and (10), respectively. Similarly, the volumetric flux in terms of the Laplace parameter  $s$ ,  $Q(y, s)$ , is obtained by adding the integrals of Eqs. (9) and (10). The solutions are as follows:

$$\tau_0(y, s) = \left. \frac{d\bar{u}_f(y, s)}{dy} \right|_{y=0} = \frac{U_i}{\sqrt{s} \sinh(d\sqrt{s})} - \frac{\cosh(d\sqrt{s})}{\sqrt{s} \sinh(d\sqrt{s})} \tag{12}$$

$$\tau_1(y, s) = \left. \frac{d\bar{u}_p(y, s)}{dy} \right|_{y=1} = \frac{U_i F}{s \sinh(F(d-1))} \tag{13}$$

$$Q(y, s) = \int_0^d \bar{u}_f(y, s) + \int_d^1 \bar{u}_p(y, s) = \frac{(U_i + 1) (\cosh(d\sqrt{s}) - 1)}{s\sqrt{s} \sinh(d\sqrt{s})} + \frac{U_i}{s \sinh(F(d-1))} \left( \frac{1 - \cosh(F(d-1))}{F} \right) \tag{14}$$

The solutions are converted to time domain by applying the Riemann-sum approximation stated in Eq. (11).

### 2.2 Validation of the Method

In order to validate the accuracy of the Riemann-sum approximation method, we set out to find the solution of the steady-state velocity analytically, which should coincide with the transient solution at large time. The expression for steady-state velocity distribution is obtained by setting  $\frac{\partial Q}{\partial t}$  in Eqs. (4) and (5) to zero. We now obtain the following ordinary differential equations:

$$\frac{d^2 u_f}{dy^2} = 0 \tag{15}$$

$$\gamma \frac{d^2 u_p}{dy^2} - \frac{u_p}{Da} = 0 \tag{16}$$

**Table 1** Numerical values of the steady-state velocity obtained using the Riemann-sum approximation method, exact solution and implicit finite difference method when  $Da = 0.1$ ,  $\beta = 0.7$ ,  $\gamma = 1.0$ ,  $d = 0.5$

| y   | Velocity    |                |                            |
|-----|-------------|----------------|----------------------------|
|     | Riemann-sum | Exact solution | Implicit finite difference |
| 0.2 | 0.7045      | 0.7045         | 0.7046                     |
| 0.4 | 0.4090      | 0.4090         | 0.4091                     |
| 0.6 | 0.1830      | 0.1830         | 0.1831                     |
| 0.8 | 0.0758      | 0.0758         | 0.0759                     |

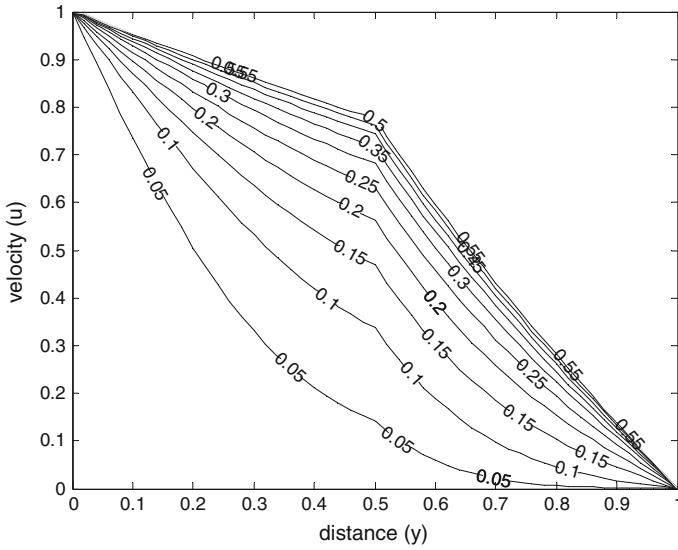


**Fig. 2** Velocity profile showing the effect of  $t$  ( $Da = 1.0, d = 0.5, \beta = -0.7, \gamma = 0.5$ )

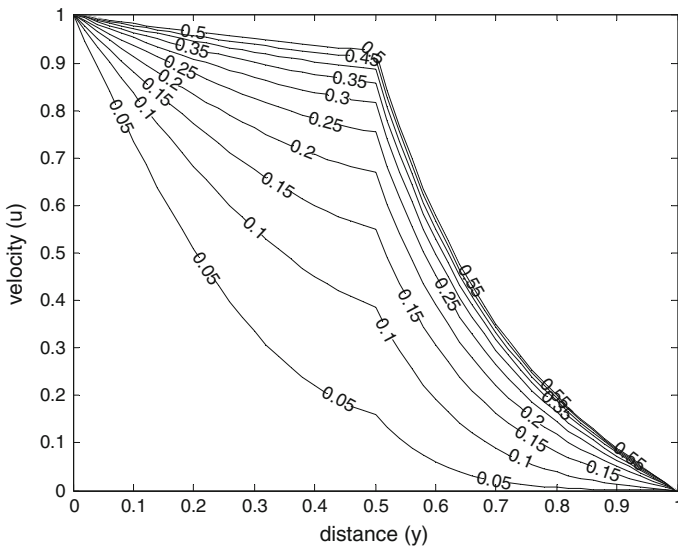


**Fig. 3** Velocity profile showing the effect of  $t$  ( $Da = 1.0, d = 0.5, \beta = -0.7, \gamma = 0.5$ )

The solution of (15) and (16) using the boundary conditions stated in (6) is

$$u_f = \frac{U_i y}{d} - \frac{y}{d} + 1 \tag{17}$$

$$u_p = \frac{U_i \sinh(\alpha(y - 1))}{\sinh(\alpha(d - 1))}, \tag{18}$$

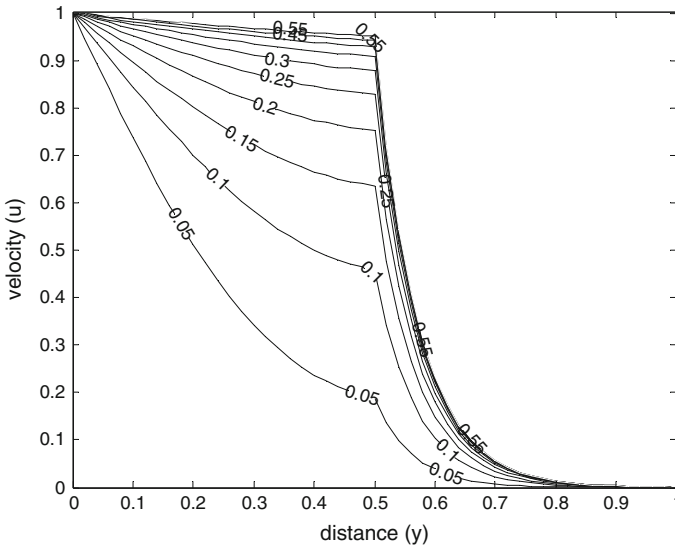


**Fig. 4** Velocity profile showing the effect of  $t$  ( $Da = 0.01, d = 0.5, \beta = -0.7, \gamma = 0.5$ )

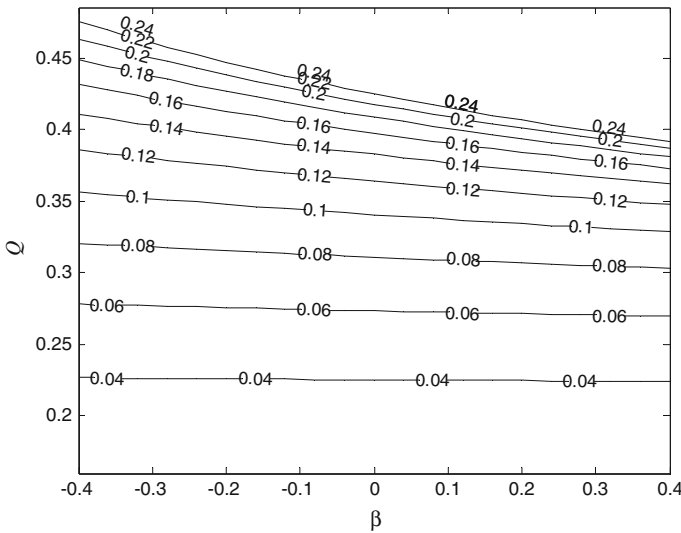


**Fig. 5** Profile of volumetric flux showing the effect of different values of  $t$  and  $\beta$  ( $d = 0.5, Da = 0.1, \gamma = 0.5$ )

where

$$\alpha = \sqrt{\frac{1}{\gamma Da}}; \quad x_7 = U_i \left( \frac{\gamma \alpha \cosh(\alpha(d-1))}{\sinh(\alpha(d-1))} - \frac{1}{d} - \frac{\beta}{\sqrt{Da}} \right); \quad U_i = -\frac{1}{dx_7}$$

The numerical results obtained for velocity using the Riemann-sum approximation method are found to be in excellent agreement with exact solutions obtained from solving Eq. (9) and (10) analytically when time is large as shown in Table 1. Furthermore, solving Eqs. (4)



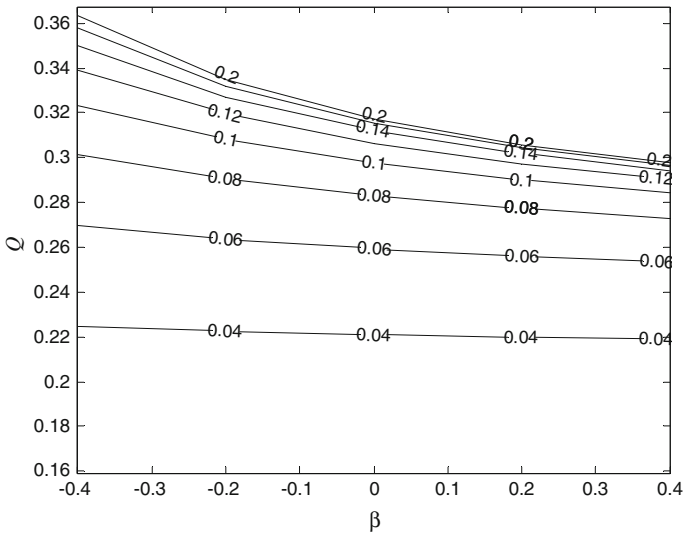


**Fig. 6** Profile of volumetric flux showing the effect of different values of  $t$  and  $\beta$  ( $d = 0.5$ ,  $Da = 0.01$ ,  $\gamma = 0.5$ )

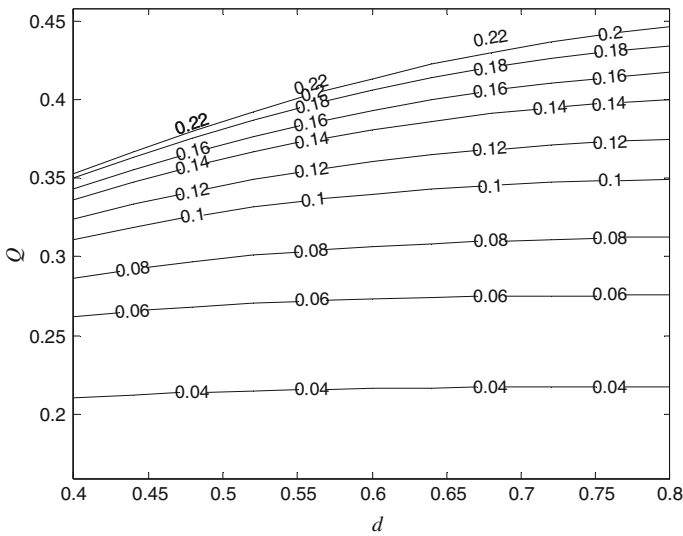
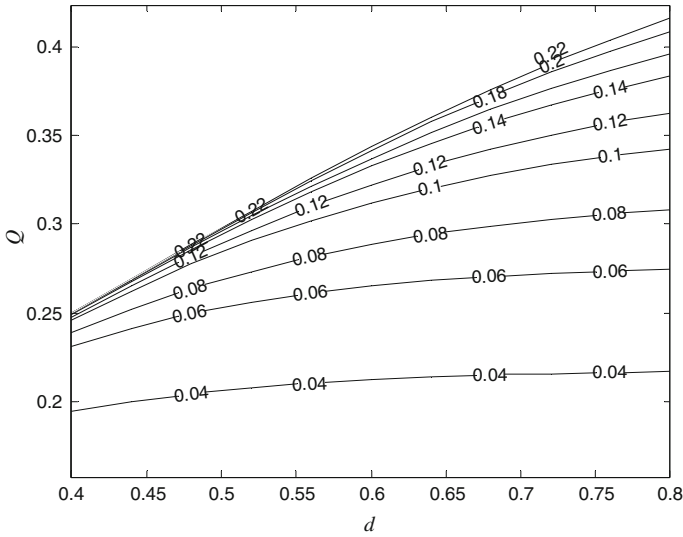


**Fig. 7** Profile of volumetric flux showing the effect of  $t$  and  $d$  ( $\beta = 0.4$ ,  $Da = 0.1$ ,  $\gamma = 0.5$ )

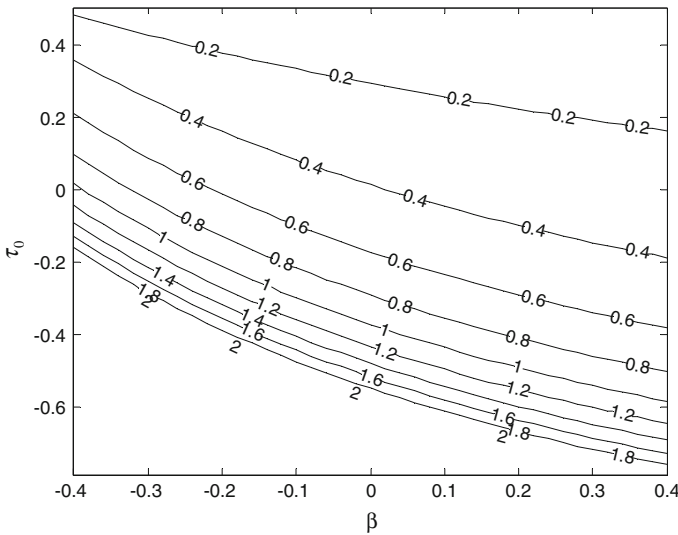
and (5) numerically using implicit finite difference method results in numerical values that agree with those obtained using Riemann-sum approximation method as shown in Table 1.

### 3 Results and Conclusions

MATLAB program is written to compute and generate line graphs for velocity, skin friction at both plates, and volumetric flux for different values of the dimensionless parameters so as to comment on their relative significance in the flow formation.

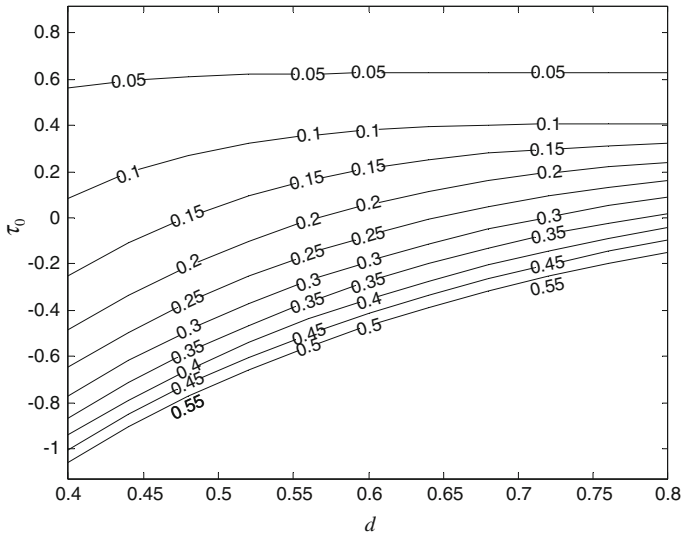


**Fig. 8** Profile of volumetric flux showing the effect of  $t$  and  $d$  ( $\beta = 0.4$ ,  $Da = 0.01$ ,  $\gamma = 0.5$ )

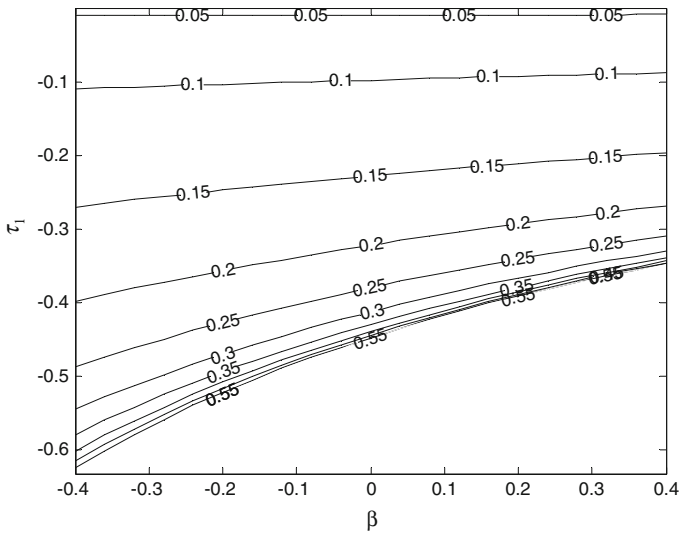


**Fig. 9** Profile of skin friction at  $y = 0$ ,  $\tau_0$  showing the effect of  $t$  and  $\beta$  ( $Da = 0.1$ ,  $d = 0.5$ ,  $\gamma = 0.5$ )

The variation of velocity with time,  $t$  is illustrated in Figs. 2, 3, and 4 when Darcy number,  $Da$  is 1.0, 0.1, and 0.01, respectively. It is observed that for different values of  $Da$ , velocity increases with  $t$ . However, the rate of increase becomes smaller as  $t$  increases and finally steady state is reached. As  $Da$  increases, porous region becomes more permeable and this increase in permeability allows greater fluid motion in the porous region. A decrease in Darcy number therefore results in a decrease in velocity and steady state is reached faster for smaller value of  $Da$ . This agrees with the finding of Kuznetsov (1997) who presented an exact solution for steady flow formation in composite channel.



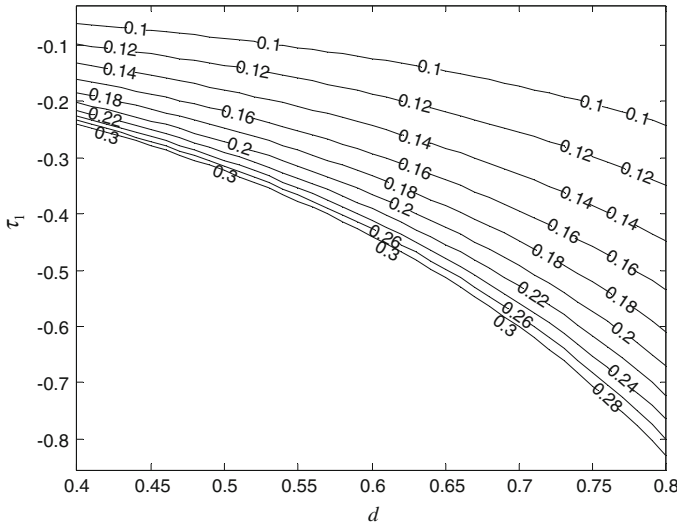
**Fig. 10** Profile of skin friction at  $y = 0$ ,  $\tau_0$  showing the effect of  $t$  and  $d$  ( $Da = 0.1$ ,  $\beta = 0.4$ ,  $\gamma = 0.5$ )



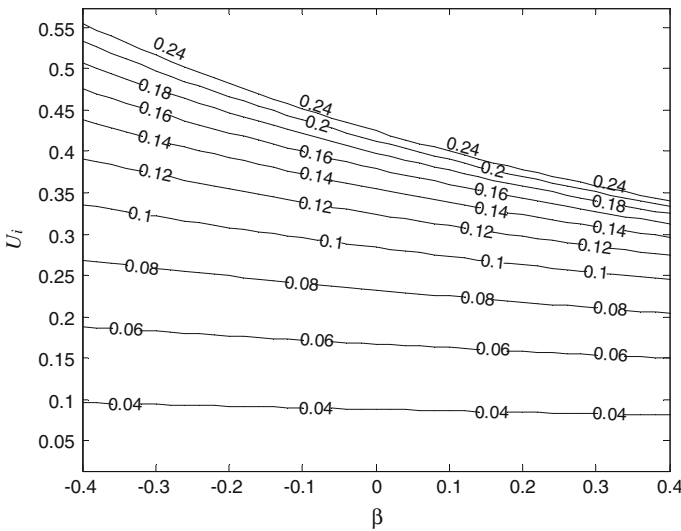
**Fig. 11** Profile of skin friction at  $y = 1$ ,  $\tau_1$  showing the effect of  $t$  and  $\beta$  ( $Da = 0.1$ ,  $d = 0.5$ ,  $\gamma = 0.5$ )

Figures 5 and 6 depict volumetric flux,  $Q$  for different  $t$  and the adjustable coefficient in the stress jump boundary condition,  $\beta$  when  $Da = 0.1$  and  $0.01$ , respectively. It is observed that  $Q$  increases as  $t$  increases but decreases as  $\beta$  increases. Steady state  $Q$  is reached faster with reduction in the value of  $Da$ .

As  $d$  increases, thickness of clear fluid region increases and thickness of porous region decreases. From Figs. 7 and 8, it is clear that as  $d$  increases,  $Q$  increases. The increase is more obvious as time increases. This is physically true because as  $d$  increases, the thickness of the porous layer decreases and hence flow experiences less resistance. The rate of increase



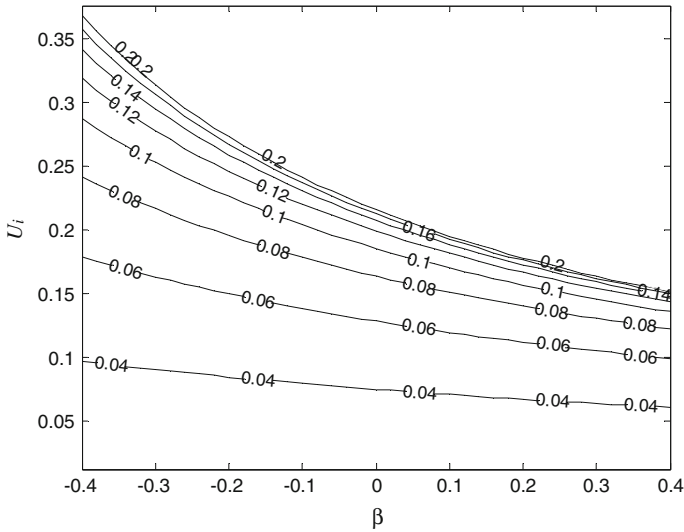
**Fig. 12** Profile of skin friction at  $y = 1$   $\tau_1$  showing the effect of  $t$  and  $d$  ( $Da = 0.1, \beta = 0.4, \gamma = 0.5$ )



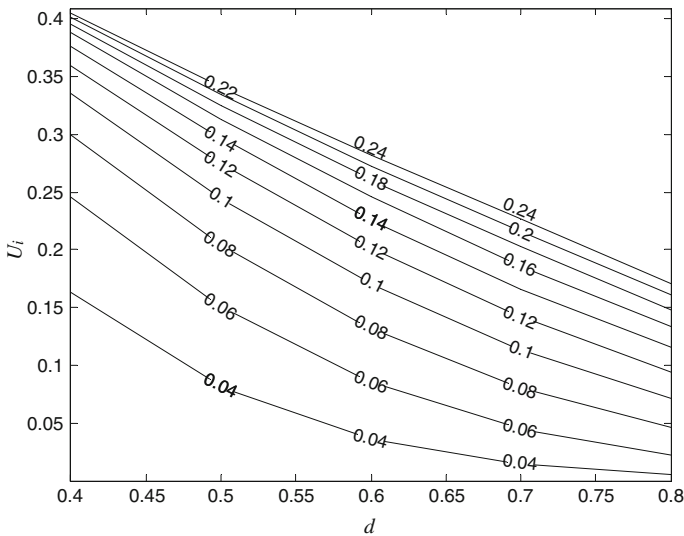
**Fig. 13** Profile of interfacial velocity,  $U_i$  showing the effect of  $t$  and  $\beta$  ( $Da = 0.1, d = 0.5, \gamma = 0.5$ )

in  $Q$  is more significant in Fig. 7 than in Fig. 8 at high value of  $t$  because of the reduction in the value of  $Da$ .

Figure 9 shows variation in skin friction,  $\tau_0$ , at  $y = 0$ , with respect to  $t$  and  $\beta$ . It is observed that  $\tau_0$  decreases as  $t$  increases. It is also noticed that  $\beta$  suppresses  $\tau_0$  at the moving plate since  $\tau_0$  decreases as  $\beta$  increases. Variation of  $\tau_0$  with  $d$  is shown in Fig. 10, where  $\tau_0$  increases as  $d$  increases. Thus a thin porous layer induces high-fluid velocity resulting in larger skin friction at the plate  $y = 0$ . In both Figs. 9 and 10,  $\tau_0$  decreases as  $t$  increases and finally, steady state is reached.



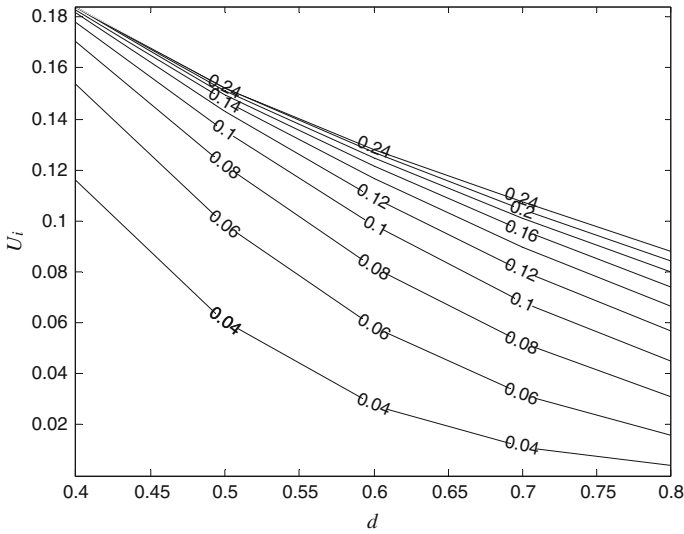
**Fig. 14** Profile of interfacial velocity,  $U_i$  showing the effect of  $t$  and  $\beta$  ( $Da = 0.01, d = 0.5, \gamma = 0.5$ )



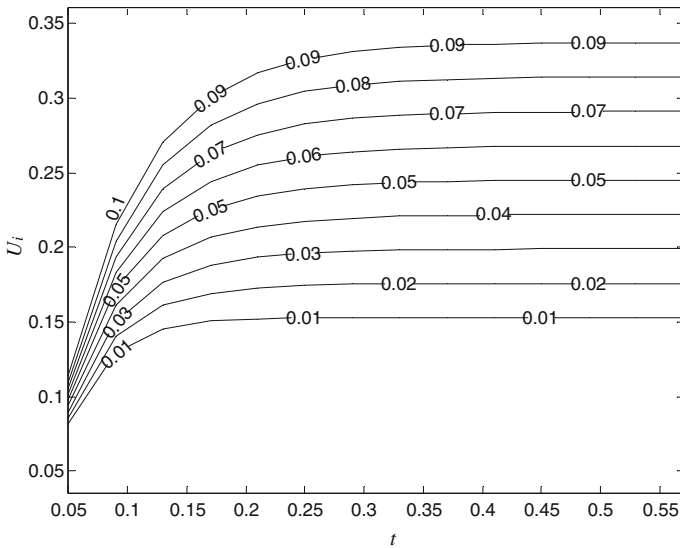
**Fig. 15** Profile of interfacial velocity,  $U_i$  showing the effect of  $t$  and  $d$  ( $Da = 0.1, \beta = 0.4, \gamma = 0.5$ )

Figure 11 shows the effect of  $t$  and  $\beta$  on skin friction  $\tau_1$ , at  $y = 1$ . It is observed that  $\tau_1$  increases as  $\beta$  increases. The increase is more prominent as  $t$  increases. In Fig. 12, decrease in  $\tau_1$  is noticed as  $d$  increases. Increase in time results in a decrease in  $\tau_1$ . Comparing Fig. 9 with Fig. 11, steady state is reached faster at the plate  $y = 1$  than the plate  $y = 0$ .

The combined effect of  $t$  and  $\beta$  on interfacial velocity,  $U_i$  is depicted in Figs. 13 and 14 for  $Da = 0.1$  and  $0.01$ , respectively. It can be seen that  $U_i$  increases as  $t$  increases but decreases as  $\beta$  increases. This effect of  $\beta$  follows a similar trend as observed by



**Fig. 16** Profile of interfacial velocity,  $U_i$  showing the effect of  $t$  and  $d$  ( $Da = 0.01, \beta = 0.4, \gamma = 0.5$ )



**Fig. 17** Profile of interfacial velocity,  $U_i$  showing the effect of  $t$  and  $Da$  ( $d = 0.5, \beta = 0.4, \gamma = 0.5$ )

Kuznetsov (1996) who considered steady-state interfacial fluid flow.  $U_i$  also decreases as  $d$  decreases. This is shown in Figs. 15 and 16. Steady state is reached faster for smaller value of  $Da$ .

The effect of  $Da$  on  $U_i$  is shown in Fig. 17. For each value of  $Da$ ,  $U_i$  increases as time increases until the steady state is reached. Also an increases in  $Da$  increases the interface velocity,  $U_i$ .

## 4 Conclusion

An unsteady Couette flow formation in a composite channel partially filled with porous material is considered. Laplace Transform technique is used to solve the governing equations, while the Riemann-sum approximation method is used to invert the Laplace domain solution to the time-domain solution. The results obtained at large time using the Riemann-sum approximations method agree considerably with steady-state results derived exactly and that obtained numerically using implicit finite difference method, demonstrating the reliability of the Riemann-sum approximation method.

The roles of  $t$ ,  $d$ ,  $Da$ ,  $\beta$ , on velocity, skin friction, and volumetric flux are investigated. We conclude that the effect of time is significant in determining fluid velocity. Velocity increases with time for each value of the parameters considered. However, because the porous region creates resistance to the fluid flow, the fluid velocity decreases with distance away from the moving plate. Skin friction decreases, while volumetric flux increases as time increases. The value of  $\beta$  and  $d$  is significant in determining skin friction, volumetric flux, and interfacial velocity.

## References

- Al-Nimr, M.A., Alkam, M.K.: Unsteady non-Darcy fluid flow in parallel-plates channels partially filled with porous materials. *Heat Mass Transf.* **33**, 315–318 (1998)
- Beavers, G.S., Joseph, D.D.: Boundary conditions at a naturally permeable wall. *J. Fluid Mech.* **30**, 197–207 (1967)
- Bhargava, S.K., Sacheti, N.C.: Heat transfer in generalized couette flow of two immiscible Newtonian fluids through a porous channel; use of Brinkman model. *Indian J. Technol.* **27**, 211–214 (1989)
- Daskalakis, J.: Couette flow through a porous medium of a high Prandtl number fluid with temperature-dependent viscosity. *Int. J. Energy Res.* **14**, 21–26 (1990)
- Hajjipour, M., Dehkordi, A.M.: Mixed convection in a vertical channel containing porous and viscous fluid regions with viscous dissipation and inertial effects: A perturbation solution. *J. Heat Transf.* **133**, 092602-1–092602-1 (2011)
- Hajjipour, M., Dehkordi, A.M.: Transient behavior of fluid flow and heat transfer in vertical channels partially filled with porous medium: Effect of inertial term and viscous dissipation. *Energy Convers. Manag.* **61**, 1–7 (2012)
- Jaballah, S., Bennacer, R., Sammouda, H., Belghith, A.: Numerical simulation of mixed convection in a channel irregularly heated partially filled with a porous medium. *J. Porous Media* **11**(3), 247–257 (2008)
- Jain, N.C., Gupta, P., Sharma, B.: Three dimensional Couette flow with transpiration cooling through porous medium in slip flow regime. *Model. Meas. Control B.* **175**(5–6), 33–52 (2006)
- Jha, B.K., Odengle, J.O., Kaurangini, M.L.: Effect of transpiration on free convective Couette flow in a composite channel. *J. Porous Media* **14**(7), 627–635 (2011)
- Khadrawi, A.F., Al-Nimr, M.A.: Unsteady natural convection fluid flow in a vertical microchannel under the effect of the Dual-Phase-Lag heat conduction model. *Int. J. Thermophys.* **28**, 1387–1400 (2007)
- Kuznetsov, A.V.: Analytical investigation of the fluid flow in the interface region between a porous medium and a clear fluid in channels partially filled with porous medium. *Appl. Sci. Res.* **56**, 53–67 (1996)
- Kuznetsov, A.V.: Influence of the stress jump condition at the porous medium/clear fluid interface on a flow at a porous wall. *Int. Commun. Heat Mass Transf.* **24**(3), 401–410 (1997)
- Kuznetsov, A.V.: Analytical investigation of Couette flow in a composite channel partially filled with a porous medium and partially with clear fluid. *Int. J. Heat Mass Transf.* **41**(16), 2556–2560 (1998)
- Muzychka, Y.S., Youanovich, M.M.: Unsteady viscous flows and Stokes' first problem. *Proc. IMECE* **14301**, 1–11 (2006)
- Neale, G., Nader, W.: Practical significance of Brinkman's extension of Darcy's law: coupled parallel flows within a channel and a bounding porous medium. *Can. J. Chem. Eng.* **52**, 475–478 (1974)
- Ochoa-Tapia, J.A., Whitaker, S.: Momentum transfer at the boundary between a porous medium and a homogeneous fluid-I: theoretical development. *Int. J. Heat Mass Transf.* **38**, 2635–2646 (1995)
- Ochoa-Tapia, J.A., Whitaker, S.: Momentum transfer at the boundary between a porous medium and a homogeneous fluid-II: comparison with experiment. *Int. J. Heat Mass Transf.* **38**, 2647–2655 (1995)

- Paul, T., Singh, A.K.: *Natural Convection Between Coaxial Vertical Cylinders Partially Filled with a Porous Material*, vol. 64. Springer, Berlin (1998)
- Paul, T., Singh, A.K., Thorpe, G.R.: Transient natural convection in a vertical channel partially filled with a porous medium. *Math. Eng. Ind.* **7**(4), 441–455 (1999)
- Singh, A.K., Gorla, R.S.R.: Heat transfer between two vertical parallel walls partially filled with a porous medium: use of a Brinkman–extended Darcy model. *Porous Media* **11**(5), 457–466 (2008)
- Singh, A.K., Pratibha, A., Singh, N.P., Singh, A.K.: Transient and non-Darcian effects on natural convection flow in a vertical channel partially filled with porous medium: Analysis with Forchheimer–Brinkman extended Darcy model. *Int. J. Heat Mass Transf.* **54**, 1111–1120 (2011)
- Tzou, D.Y.: *Macro to Micro Scale Heat Transfer: The Lagging Behaviour*. Taylor and Francis, London (1997)
- Vafai, K., Kim, S.J.: Fluid mechanics of the interface region between a porous medium and a fluid layer- an exact solution. *Int. J. Heat Fluid Flow* **11**(3), 254–256 (1990)